

# The Importance of Antipersistence for Traffic Jams

Sebastian M. Krause, Lars Habel, Thomas Guhr, and Michael Schreckenberg  
*Faculty of Physics, University of Duisburg-Essen, 47058 Duisburg, Germany*

Universal characteristics of road networks and traffic patterns can help to forecast and control traffic congestion. The antipersistence of traffic flow time series has been found for many data sets, but its relevance for congestion has been overseen. Based on empirical data from motorways in Germany, we study how antipersistence of traffic flow time-series impacts the duration of traffic congestion on a wide range of time scales. We find a large number of short lasting traffic jams, which implies a large risk for rear-end collisions.

## I. INTRODUCTION

Intraurban road networks in agglomerations and megacities often operate near or above their designed specifications in terms of e.g. maximum capacities, which leads to congestion and increases travel times [1]. Exceeding the specifications can also result in an increased wear of important parts of the network infrastructure, in particular bridges. During subsequent maintenance works, the road capacities are typically reduced, which adds to the problem. Under these circumstances, road authorities are faced with the challenge of optimal traffic assignment and control. To this end, universal characteristics of road networks and the according traffic patterns [2] can help to identify systemic bottlenecks [3]. While local traffic time series are best characterised with identifying different traffic states and state transitions [4, 5], network aspects are well represented with fractal scaling laws [2, 6, 7]. Both aspects are grounded on empiric evidence in very diverse situations and are well understood with microscopic models. Especially the spatio-temporal behaviour of traffic patterns is explained comprehensively with the three-phase traffic theory [8, 9], which distinguishes between free flow, synchronised traffic and wide moving jams. The latter two phases are summarised under the heading of congested traffic.

Empirical studies find fractal properties in local traffic time series [10–17], also based on methods like detrended fluctuation analysis (DFA) [18, 19]. These findings are consistent with results from cellular automata traffic flow models [17, 20]. Fractal modelling based on fractional Brownian motion (fBm) [21] was used for forecasting traffic flow [22]. However, the implications for traffic breakdown are not well understood up to now. This limits the implicative relevance of fractal properties for the fine-tuning of traffic models.

Here we study how the fractal nature of traffic flow time-series impacts the duration of traffic congestion. We show that the corresponding distribution is very broad. We succeed in explaining it as a consequence of antipersistence in traffic flow. For our empirical analysis, we use traffic data from inductive loops located at crosssections  $i \in \{1, \dots, 33\}$  on the Cologne orbital motorways A1, A3 and A4 in Germany, which are depicted in fig. 1. Motorway traffic in this area has also been studied in [23–25]. The data set comprises minutely aggregated traffic



FIG. 1. Locations of traffic detector crosssections  $i$  (dots) on the Cologne orbital motorway. Specific crosssections are numbered counter-clockwise. Map tiles by Stamen Design, under CC BY 3.0. Data © OpenStreetMap Contributors.

flows  $q(i, t)$ , densities  $\rho(i, t)$  and velocities  $v(i, t)$  for each minute  $t$  of the year 2015 and all crosssections  $i$ . A traffic flow  $q(i, t)$  is defined as the number of vehicles passing the crosssection  $i$  on all lanes in minute  $t$ , whereas  $v(i, t)$  denotes the corresponding averaged vehicular velocities.

## II. STATISTICS OF TRAFFIC JAMS

Fig. 2 displays velocity profiles versus time for a specific day. At crosssections 1 and 2, there is a fixed speed limit of 60 km/h. Sections 3–7 and 12–25 have fixed speed limits of at most 120 km/h, whereas sections 8–11 and 26–33 are equipped with variable speed limit signs. For crosssections with numbers larger than 25, traffic jams develop before 8:00, around 12:00 and around 16:00.

For understanding the spatio-temporal patterns shown in fig. 2, we use definitions from three-phase traffic theory. Free flow and congested traffic states can be distinguished by calculating a minimum velocity of free flow  $v_{\min}^{(\text{free})} = q_{\max}^{(\text{free})} / \rho_{\max}^{(\text{free})}$ , where  $q_{\max}^{(\text{free})}$  is the maximum free flow and  $\rho_{\max}^{(\text{free})}$  is the maximum free density [8]. Then, states with  $v(i, t) < v_{\min}^{(\text{free})}$  are considered congested. However, this separation becomes erro-

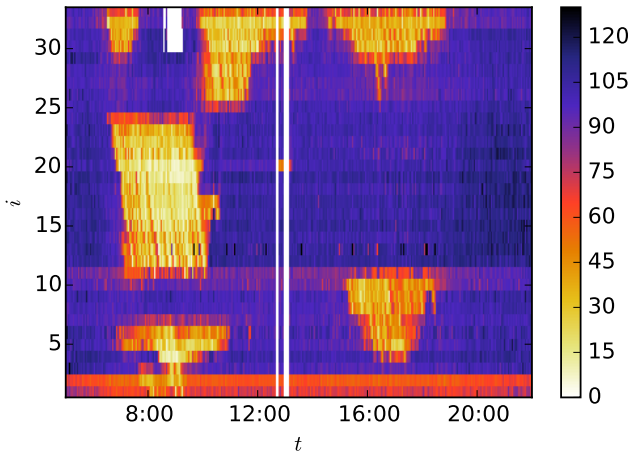


FIG. 2. Velocity profile during Wednesday, 21 October 2015 along the crosssections  $i$  specified in fig. 1. The colours indicate vehicular velocities  $v(i, t)$  in km/h, averaged over one minute windows on all possible lanes of a crosssection. The white regions due to missing data are skipped in the further data processing.

neous where speed limits change often. To identify congested traffic, we therefore consider times and crosssections with  $v(i, t) < v_{\text{jam}}$  below a fixed threshold velocity  $v_{\text{jam}} = 40$  km/h as congested.

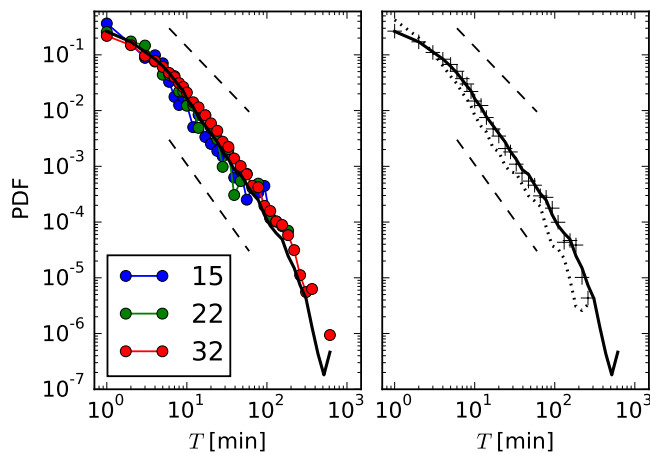


FIG. 3. Left: PDF of traffic congestion durations  $T$  for  $v_{\text{jam}} = 40$  km/h in double logarithmic plot. Symbols indicate different crosssections, the black solid line is the average over crosssections 3 to 33. For comparison, power laws  $T^{-\gamma}$  with exponent  $\gamma = 3/2$  (upper dashed line) and  $\gamma = 2$  (lower dashed line) are shown. Right: The average result (black solid line) changes only slightly for data reduced to the first three months (crosses), or for reduced  $v_{\text{jam}} = 20$  km/h (dotted line).

In fig. 3 we show the probability density function (PDF) of traffic congestion durations  $T$ . We identify a local congestion of duration  $T$ , if at a certain crosssection

$i$  we have

$$v(i, t) \geq v_{\text{jam}} \quad (1)$$

$$\text{and } v(i, t + T + 1) \geq v_{\text{jam}} \quad (2)$$

$$\text{and } v(i, \tau) < v_{\text{jam}} \quad (3)$$

for  $t < \tau \leq t + T$ . The resulting distribution is very broad. The dashed lines provide power laws  $T^{-\gamma}$  for comparison, with  $\gamma = 3/2$  and  $\gamma = 2$ . As shown, the results are qualitatively the same for different  $v_{\text{jam}}$  as well as for data reduced to the first three months. Summarising, we find a robust power-law behaviour with exponents in the range  $\gamma = 3/2$  up to  $\gamma = 2$ . A cutoff around 200 minutes results from the limited duration of rush hours. Importantly, the small exponent  $\gamma$  implies that traffic congestion durations on all scales from minutes to hours are relevant. For larger exponents, the long durations would be of minor importance.

To link congestion durations with traffic conditions leading to a traffic breakdown, we analyse traffic flow time-series and the reaction of the velocity on large flows. Traffic breakdowns occur at bottlenecks with some probability, if large traffic flows are present [8, 9]. We use a fixed threshold flow  $q_{\text{thr}}$  to calculate the breakdown probability  $P_{\text{jam}}(i, q_{\text{thr}})$  with the following algorithm: Consider all events with  $q(i, t) > q_{\text{thr}}$  and  $v(i, t) \geq v_{\text{jam}}$ , where in each of the following minutes  $\Delta t \in \{1, \dots, 5\}$  min it holds separately either

$$v(i, t + \Delta t) < v_{\text{jam}} \quad (\text{jam occurs}) \quad (4)$$

$$\text{or } v(i, t + \Delta t) \geq v_{\text{jam}} \text{ and } q(t + \Delta t) > q_{\text{thr}}. \quad (5)$$

Among these events, events with traffic breakdown have  $v(i, t + \Delta t) < v_{\text{jam}}$  for at least one  $\Delta t$ , and their fraction yields the breakdown probability  $P_{\text{jam}}$ .

In fig. 4 we present resulting breakdown probabilities for crosssections 11, 22 and 33 and varied threshold flow  $q_{\text{thr}}$ , split into time intervals of the four calendar quarters Q1, Q2, Q3 and Q4 of the year 2015. For all curves, a sharp jump can be observed. The minimum flow with breakdown probability  $P_{\text{jam}} = 1$  is denoted as  $q_{\text{max}}^{(\text{free})}$  [9]. We find  $q_{\text{max}}^{(\text{free})}$  in the range  $51 \text{ min}^{-1}$  to  $54 \text{ min}^{-1}$  for crosssection 11, in the range  $109 \text{ min}^{-1}$  to  $113 \text{ min}^{-1}$  for crosssection 22, and values from  $75 \text{ min}^{-1}$  up to  $99 \text{ min}^{-1}$  for crosssection 33. The maximum free flow  $q_{\text{max}}^{(\text{free})}$  varies strongly between the crosssections, mainly because of the different number of lanes at each section. At crosssection 33, the maximum free flow reduces strongly after the first half of the year, implying a changed lane configuration at a construction site. At other crosssections, the maximum free flow stays almost constant over the year.

Knowing that above a certain  $q_{\text{thr}}$  traffic breakdown is likely to occur within a few minutes, we further analyse, for how long traffic flow exceeds  $q_{\text{thr}}$ , but does not break down [26]. Would  $q_{\text{max}}^{(\text{free})}$  be reduced to the smaller flow  $q_{\text{thr}}$  (for example due to construction works), traffic jams would occur as long as  $q > q_{\text{thr}}$ . In fig. 5, traffic flow time series for Tuesday, 14 July 2015 are displayed. The

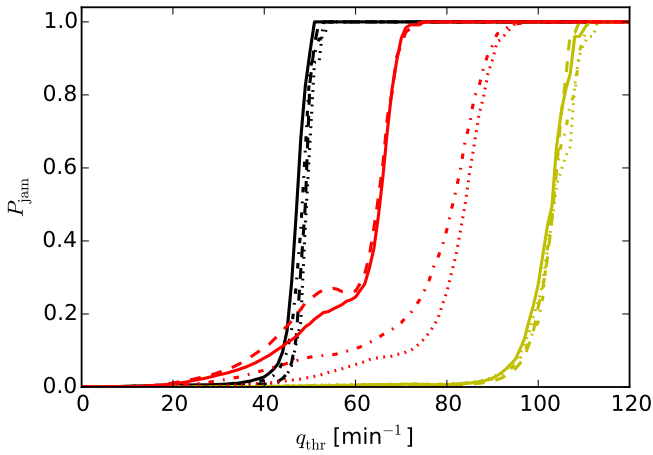


FIG. 4. Probability  $P_{\text{jam}}$  that during up to five minutes with  $q > q_{\text{thr}}$  the velocity falls below  $v_{\text{jam}}$ , versus threshold flow  $q_{\text{thr}}$ . Black lines are for crosssection 11, yellow lines for crosssection 22 and red lines for crosssection 33. Line styles are dotted for the first quarter of the year, dash-dotted for the second quarter, dashed for the third quarter and solid for the last quarter.

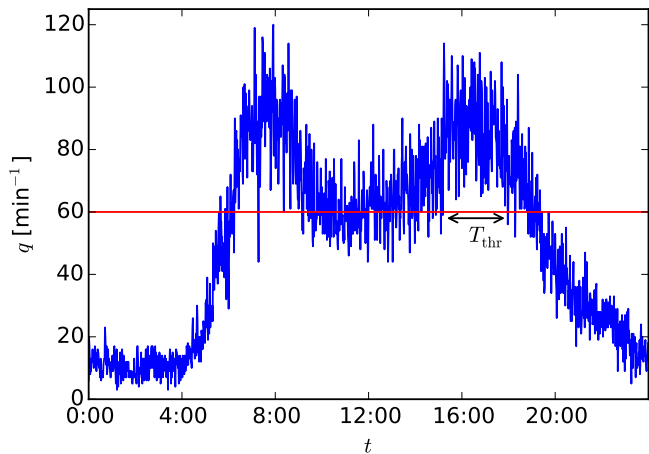


FIG. 5. Traffic flow time series  $q(t)$  for road section 22 on Tuesday, 14 July 2015. The duration  $T_{\text{thr}}$  of a period with  $q > q_{\text{thr}} = 60 \text{ min}^{-1}$  is indicated with a double arrow.

time series shows strong fluctuations for short times, and a trend with one rush hour around 8:00 and a second rush hour around 16:00. Let us assume a threshold flow of  $q_{\text{thr}} = 60 \text{ min}^{-1}$ , corresponding to the red line. We identify durations  $T_{\text{thr}}$  during which the flow exceeds a certain threshold  $q_{\text{thr}}$ , i.e.  $q > q_{\text{thr}}$ . Due to the fluctuations in  $q(t)$ , we expect shortest durations  $T_{\text{thr}}$  down to a minute. In fig. 5 the largest duration  $T_{\text{thr}}$  is highlighted with the double arrow and spans almost three hours. The PDF of  $T_{\text{thr}}$  for different crosssections and thresholds  $q_{\text{thr}}$  are shown in fig. 6. On the left, we use 263 days without a single minute of traffic jam in cross-

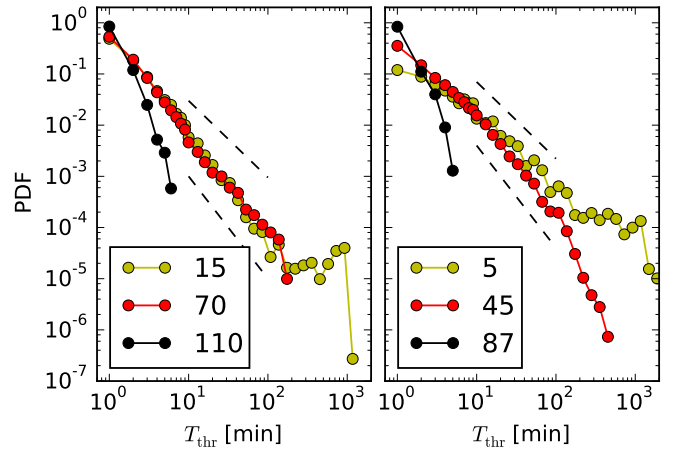


FIG. 6. PDF of durations  $T_{\text{thr}}$ , during which the flow is above a threshold,  $q > q_{\text{thr}}$ . The legends indicate different choices of  $q_{\text{thr}}$ . On the left, only days without detected congestion at crosssection 22 are considered. On the right, only days with at least four hours of congestion at crosssection 32 are considered. The dashed lines have exponents  $\gamma_{\text{thr}} = 3/2$  and  $\gamma_{\text{thr}} = 2$ .

section 22. For the threshold at the maximum free flow  $q_{\text{thr}} = q_{\text{max}}^{(\text{free})} = 110 \text{ min}^{-1}$  (black symbols), longer durations are not seen. This is because here we restricted the data to days without traffic jam. Longer durations with such high flow would result in a traffic jam. For a smaller threshold  $q_{\text{thr}} = 70 \text{ min}^{-1}$  (red symbols) we see a power law distribution of durations  $\propto (T_{\text{thr}})^{-\gamma_{\text{thr}}}$ , with exponent close to  $\gamma_{\text{thr}} = 2$ . Were the critical flow reduced to the smaller flow (for example due to reconstruction works), the durations  $T_{\text{thr}}$  would translate into traffic jam durations  $T$ . The PDF of traffic jam durations shows a power law with exponent close to  $\gamma = 2$ , cf. fig. 3. This result supports the interpretation that durations  $T_{\text{thr}}$  of the traffic flow  $q(t)$  being above a threshold explain the distribution of traffic jam durations  $T$ . Only short traffic jam durations  $T$  are suppressed compared to short  $T_{\text{thr}}$ . This is because the traffic needs some time to break down. For small threshold  $q_{\text{thr}} = 15 \text{ min}^{-1}$ , the longest duration  $T_{\text{thr}}$  can be as long as the whole working day, resulting in a peak at about 600 min or ten hours. To illustrate that these statistical features of traffic flow are not altered if the velocity breaks down, we consider 139 days with at least four hours with  $v < v_{\text{jam}}$  a day, in the second half of 2015 in crosssection 32. Results are shown on the right of fig. 6.

### III. EXPLANATION

To understand the durations  $T_{\text{thr}}$  with  $q > q_{\text{thr}}$ , we compare them with fractional Brownian motion (fBm) [21]. We denote the fBm random function as  $B_H(t)$  with Hurst exponent  $0 < H < 1$  and dimensionless

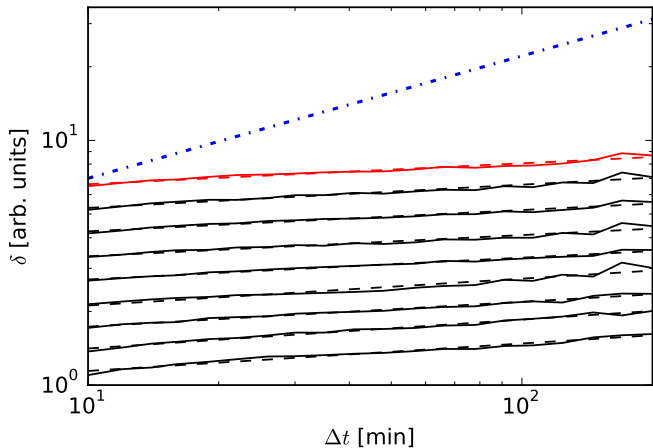


FIG. 7. Detrended standard deviation  $\delta$  of the flow time series  $q(t)$  vs. size of the sub-samples  $\Delta t$ . The red line corresponds to fig. 5, black lines to flow time series on different times and crosssections. The blue dash-dotted line with exponent  $1/2$  corresponds to Brownian motion.

time  $\tilde{t}$ . The defining property of the fBm with  $B_H(0) = 0$  is its dependency structure [21] for times  $\tilde{t}, \tilde{s} \geq 0$ ,

$$2 \langle B_H(\tilde{t})B_H(\tilde{s}) \rangle = \tilde{t}^{2H} + \tilde{s}^{2H} - |\tilde{t} - \tilde{s}|^{2H}, \quad (6)$$

where  $\langle \rangle$  is the ensemble average over realisations.

The PDF of durations  $T_{\text{fBm}}$  during which the time series exceeds a certain threshold  $B_{\text{thr}}$ , i.e.  $B_H(\tilde{t}) > B_{\text{thr}}$ , is known to scale with a power law as  $(T_{\text{fBm}})^{-\gamma_{\text{fBm}}}$  with  $\gamma_{\text{fBm}} = 2 - H$  [27]. The traffic flow time series in fig. 5 shows strong fluctuations on short time scales, and thus antipersistent, i.e. non-Markovian, behaviour with anti-correlated increments and Hurst exponent  $H < 1/2$  [21]. Another implication of antipersistent fBm is a subdiffusive behaviour, with variance increasing sub-linear in time as

$$\langle (B_H(\tilde{t} + \Delta\tilde{t}) - B_H(\tilde{t}))^2 \rangle = |\Delta\tilde{t}|^{2H}. \quad (7)$$

This result can be derived from eq. (6). For small  $H$  it implies that changes are large on short times and stagnating for longer times. The time dependence of the variance can be used for estimating  $H$  from flow time series  $q(t)$ . To deal with the trend in the signal with pronounced rush hours, we use detrended fluctuation analysis (DFA) [18, 19]. We divide the time series  $q(t)$  of the day into sub-samples of length  $\Delta t$  and correct the linear trend in each sample. Then we calculate the standard deviation in each sub-sample, and average over all sub-samples, to obtain the average standard deviation  $\delta$ . We repeat this procedure for different  $\Delta t$ . In fig. 7 we show how the detrended standard deviation  $\delta$  depends on the sub-sample size  $\Delta t$ . The red solid line corresponds to fig. 5. According to [19], the sub-sample size should be chosen larger than 10 elements and smaller than about  $1/4$  of the full sample size. The Hurst exponent  $H$  can

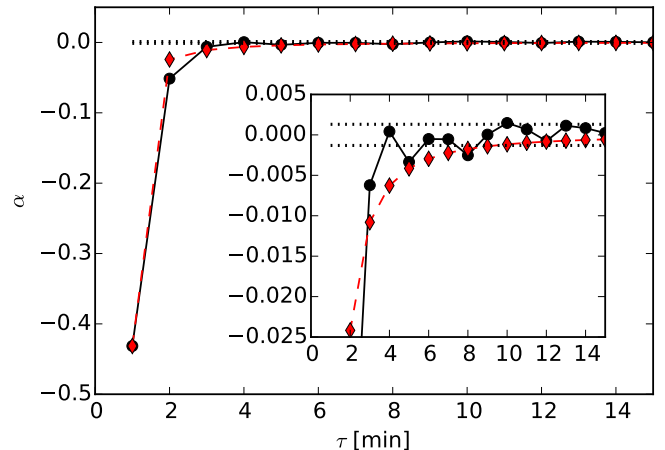


FIG. 8. Autocorrelation  $\alpha$  over time lag  $\tau$  of one-minute increments of the flow  $q$  averaged over all days and crosssections (black circles) compared with fBm with  $H = 0.093$  (red diamonds). Horizontal dotted lines indicate the interval spanned by shuffled data. The inset represents an enlarged part of the main figure.

be identified as the slope of the linear fit in the log-log plot [19]. For the red curve we find  $H = 0.085$ . Other examples for different days and crosssections 15 and 32 are shifted for better visibility. The dash-dotted line with exponent  $1/2$  corresponds to Brownian motion. With  $H < 1/2$  we find strong subdiffusive behaviour in a range from ten minutes up to three hours. Performing DFA for single days on all crosssections, we find Hurst exponents between 0.038 and 0.24, with mean 0.088 and standard deviation 0.028. Days with more than ten minutes of missing data are neglected. For the Kerner-Klenov-Wolf cellular automaton three-phase traffic flow model, antipersistent behaviour of the free traffic density is reported in [20]. With the use of DFA, Hurst exponents down to  $H = 0.1$  are found in synthetic data. An analysis of real world data finds Hurst exponents around  $H = 0.17$  for free flow traffic [10]. Another study finds persistence in real traffic data, however the data is not detrended there [11].

To understand the time evolution of  $q(t)$ , let us assume we identified the non-stochastic trend  $\mu(t)$  and propose the model  $q_m$ , defined as

$$q_m(t + \Delta t) - q_m(t) = \mu(t + \Delta t) - \mu(t) + \sigma(t) \left[ B_H \left( \frac{t}{t_0} + \frac{\Delta t}{t_0} \right) - B_H \left( \frac{t}{t_0} \right) \right]. \quad (8)$$

The time dependent function  $\sigma(t)$  is needed to adapt the physical dimension and to account for a slowly varying time dependence of the fluctuation strength. For the time scale  $t_0$  we can use one minute. For  $H$ , we insert the Hurst exponent as found empirically around  $H = 0.1$ . For  $H \neq 1/2$ , the increments  $B_H(\tilde{t} + \Delta\tilde{t}) - B_H(\tilde{t})$  are dependent for different  $\tilde{t} =$

$n\Delta\tilde{t}$ . Therefore, the numerical generation of time series is not as straight forward as for standard Brownian motion. We find a strong negative autocorrelation  $\alpha(\tau) = [\langle \Delta q(t+\tau)\Delta q(t) \rangle_t - \langle \langle \Delta q(t) \rangle_t \rangle^2] / \langle \langle \Delta q(t) \rangle_t \rangle^2$  of one minute increments  $\Delta q(t) = q(t+1) - q(t)$  for short time lags  $\tau$ , see the black circles in fig. 8. Results are averaged over all road sections and all days with at most ten minutes of missing data. For larger time lags  $\tau$ , the autocorrelation is dominated by noise. This result is consistent with antipersistent fBm, as can be found with eq. 6. The red diamonds show results for  $H = 0.093$ . This Hurst exponent is also in good agreement with results from DFA, see fig. 7. Notice that non-stochastic increments of the form  $\mu(t+1) - \mu(t)$  are small compared to fluctuations on short time scales, what allows us to investigate the autocorrelation of  $q$  without subtracting the non-stochastic part.

Based on the model  $q_m$ , we now investigate the durations  $T_{\text{thr}}$  with  $q_m > q_{\text{thr}}$ . For fBm, a power law with exponent  $\gamma_{\text{fBm}} = 2 - H$  was reported in [27]. In our case, we find  $\gamma_{\text{fBm}} = 2 - H \approx 1.9$ , which is in good agreement with the empirical findings for  $\gamma_{\text{thr}}$  in fig. 6. For fBm, it was further found that the power law behaviour is even present with an additional drift-like term [27]. In this case, for negative drift there is a cut-off at large times, what is also consistent with our empirical results, see for example the red circles on the right of fig. 6. For positive drift, the PDF at long durations  $T$  with  $q_m > q_{\text{thr}}$  are increased. We see this effect in real data in fig. 6 for small  $q_{\text{thr}}$ , the yellow circles. In our model  $q_m(t)$ , the drift  $\mu(t)$  would be a function depending on the time of the day, the day of the week and further factors. However, the identification of this drift term goes beyond the scope of this study. Moreover, let us compare with scaling in other socio-economic fields. Burst- and inter-burst durations  $T$  in currency exchange markets have been found to scale as  $T^{-3/2}$  [28]. This hints at normal diffusion and Markovian behaviour. Examples of scaling in systems which are not tuned to a phase transition are also known in the context of coherent noise [29], what holds implications for adaptive electricity markets [30].

#### IV. CONCLUSION

First, our results strongly corroborate the anti-persistent behaviour of traffic flow time series  $q(t)$ : The Hurst exponent around  $H = 0.1$  from DFA, negative autocorrelations of one minute increments hinting at Hurst exponent around  $H = 0.09$ , and finally a power law  $T^{-\gamma_{\text{thr}}}$  for durations  $T_{\text{thr}}$  above thresholds  $q > q_{\text{thr}}$  with exponent around  $\gamma_{\text{thr}} = 2$ . The latter is connected with a Hurst exponent  $H = 2 - \gamma_{\text{thr}}$  close to zero, and therefore strongly in the antipersistent regime. Taking all findings together, we found a robust universal property of traffic flow, which can be observed on different road sections, at different times and with or without long times of congestion. Second, we showed that congestion durations  $T$  are distributed in the same way as durations  $T_{\text{thr}}$  of the flow above threshold. With identifying critical thresholds of the flow  $q_{\text{thr}}$  for our traffic data, we concluded that the durations  $T_{\text{thr}}$  translate into traffic jam durations  $T$ . This led us, third, to our main result that antipersistence in traffic flow is a crucial property for understanding patterns of traffic congestion.

The broad distribution of traffic jam durations  $T$  has implications for how traffic jams can be characterised. This is relevant for navigation systems with congestion warning. Especially short lasting traffic jams bare a large risk for rear-end collisions. Also, traffic models can benefit from our findings.

#### ACKNOWLEDGMENTS

We thank Strassen.NRW for providing the empirical traffic data. LH and MS have been supported by Deutsche Forschungsgemeinschaft (DFG) within the Collaborative Research Center SFB 876 “Providing Information by Resource-Constrained Analysis”, project B4 “Analysis and Communication for the Dynamic Traffic Prognosis”.

- 
- [1] ECMT, *Managing Urban Traffic Congestion* (OECD Publishing, 2007).
  - [2] Marko Popović, Hrvoje Štefančić, and Vinko Zlatić, “Geometric origin of scaling in large traffic networks,” *Phys. Rev. Lett.* **109**, 208701 (2012).
  - [3] Daqing Li, Bowen Fu, Yunpeng Wang, Guangquan Lu, Yehiel Berezin, H. Eugene Stanley, and Shlomo Havlin, “Percolation transition in dynamical traffic network with evolving critical bottlenecks,” *Proc. Nat. Acad. Sci.* **112**, 669–672 (2015).
  - [4] Bhagwant Persaud, Sam Yagar, and Russel Brownlee, “Exploration of the Breakdown Phenomenon in Freeway Traffic,” *Transp. Res. Rec.* **1634**, 64–69 (1998).
  - [5] Boris S. Kerner, “Empirical macroscopic features of spatial-temporal traffic patterns at highway bottlenecks,” *Phys. Rev. E* **65**, 46138 (2002).
  - [6] Giovanni Petri, Paul Expert, Henrik J Jensen, and John W Polak, “Entangled communities and spatial synchronization lead to criticality in urban traffic.” *Sci. Rep.* **3**, 1798 (2013).
  - [7] Marc Barthélemy, “Spatial networks,” *Phys. Rep.* **499**, 1–101 (2011).
  - [8] Boris S. Kerner, *The Physics of Traffic: Empirical Free-way Pattern Features, Engineering Applications, and Theory* (Springer, 2004).
  - [9] Boris S. Kerner, *Introduction to Modern Traffic Flow Theory and Control: The Long Road to Three-Phase Traffic Theory* (Springer, 2009).
  - [10] Sheng Peng, Wang Jun-Feng, Tang Tie-Qiao, and Zhao Shu-Long, “Long-range correlation analysis of urban traf-

- fic data,” *Chinese Phys. B* **19**, 080205 (2010).
- [11] Matthew G Karlaftis and Eleni I Vlahogianni, “Memory properties and fractional integration in transportation time-series,” *Transport. Res. C* **17**, 444–453 (2009).
- [12] BA Toledo, V Munoz, J Rogan, C Tenreiro, and Juan Alejandro Valdivia, “Modeling traffic through a sequence of traffic lights,” *Phys. Rev. E* **70**, 016107 (2004).
- [13] Pengjian Shang, Meng Wan, and Santi Kama, “Fractal nature of highway traffic data,” *Comp. Math. Appl.* **54**, 107–116 (2007).
- [14] Xuewei Li and Pengjian Shang, “Multifractal classification of road traffic flows,” *Chaos, Solitons & Fractals* **31**, 1089–1094 (2007).
- [15] Xuejiao Wang, Pengjian Shang, and Jintang Fang, “Traffic time series analysis by using multiscale time irreversibility and entropy,” *Chaos* **24**, 032102 (2014).
- [16] Jan W. Kantelhardt, Matthew Fullerton, Mirko Kämpf, Cristina Beltran-Ruiz, and Fritz Busch, “Phases of scaling and cross-correlation behavior in traffic,” *Physica A* **392**, 5742–5756 (2013).
- [17] Thomas Zaksek and Michael Schreckenberg, “Fractal Analysis of Empirical and Simulated Traffic Time Series,” in *Traffic Granul. Flow '15*, edited by Victor L. Knoop and Winnie Daamen (Springer, 2016) pp. 435–442.
- [18] Chung-Kang Peng, Sergey V. Buldyrev, Shlomo Havlin, Michael Simons, H. Eugene Stanley, and Ary L. Goldberger, “Mosaic organization of dna nucleotides,” *Phys. Rev. E* **49**, 1685 (1994).
- [19] Jan W. Kantelhardt, Stephan A. Zschiegner, Eva Koscielny-Bunde, Shlomo Havlin, Armin Bunde, and H. Eugene Stanley, “Multifractal detrended fluctuation analysis of nonstationary time series,” *Physica A* **316**, 87–114 (2002).
- [20] J. J. Wu, H. J. Sun, and Z. Y. Gao, “Long-range correlations of density fluctuations in the kerner-klenov-wolf cellular automata three-phase traffic flow model,” *Phys. Rev. E* **78**, 036103 (2008).
- [21] Benoit B. Mandelbrot and John W. Van Ness, “Fractional brownian motions, fractional noises and applications,” *SIAM Review* **10**, 422–437 (1968).
- [22] Jacques Lévy-Vehel, Robert Vojak, and Mehdi Danesh-Pajouh, “Multifractal description of road traffic structure,” in *7th IFAC/IFORS Symposium on Transportation Research*, edited by B. Liu and J. M. Blosseville (Pergamon, 1995).
- [23] Lutz Neubert, Ludger Santen, Andreas Schadschneider, and Michael Schreckenberg, “Single-vehicle data of highway traffic: A statistical analysis,” *Phys. Rev. E* **60**, 6480–6490 (1999).
- [24] Ihor Lubashevsky, Reinhard Mahnke, Peter Wagner, and Sergey Kalenkov, “Long-lived states in synchronized traffic flow: Empirical prompt and dynamical trap model,” *Phys. Rev. E* **66**, 016117 (2002).
- [25] Denis Belomestny, Volker Jentsch, and Michael Schreckenberg, “Completion and continuation of non-linear traffic time series: a probabilistic approach,” *J. Phys. A Math. Gen.* **36**, 11369 (2003).
- [26] Florian Knorr, Thomas Zaksek, Johannes Brüggemann, and Michael Schreckenberg, “Statistical Analysis of High-Flow Traffic States,” in *Traffic Granul. Flow '13*, edited by Mohcine Chraïbi, Maik Boltes, Andreas Schadschneider, and Armin Seyfried (Springer, 2015) pp. 557–562, arXiv:arXiv:1312.3589v1.
- [27] Mingzhou Ding and Weiming Yang, “Distribution of the first return time in fractional brownian motion and its application to the study of on-off intermittency,” *Phys. Rev. E* **52**, 207 (1995).
- [28] V Gontis and A Kononovicius, “Burst and inter-burst duration statistics as empirical test of long-range memory in the financial markets,” arXiv preprint arXiv:1701.01255 (2017).
- [29] MEJ Newman and Kim Sneppen, “Avalanches, scaling, and coherent noise,” *Phys. Rev. E* **54**, 6226 (1996).
- [30] Sebastian M. Krause, Stefan Börries, and Stefan Bornholdt, “Econophysics of adaptive power markets: When a market does not dampen fluctuations but amplifies them,” *Phys. Rev. E* **92**, 012815 (2015).